

Peak effect, melting, and transport in skyrmion crystalsC. Reichhardt and C. J. O. Reichhardt *Theoretical Division and Center for Nonlinear Studies, Los Alamos National Laboratory, Los Alamos, New Mexico 87545, USA*

(Received 1 April 2023; accepted 7 July 2023; published 25 July 2023)

We numerically examine the transport of skyrmions driven over weak random quenched disorder using a modified Thiele approach that includes the thermal softening of skyrmion pairwise interactions introduced by Wang *et al.* [*Phys. Rev. Appl.* **18**, 044024 (2022)]. The depinning transition is elastic at low temperatures but becomes plastic with a reduced threshold at higher temperatures due to the competition between thermal creep and thermal softening, indicating a temperature-induced order to disorder transition into a glass state. The resulting nonmonotonic critical depinning forces and crossing of the velocity-force curves are similar to what is observed in the peak effect for type-II superconducting vortex lattices, where the softening of vortex-vortex interactions with temperature leads to an order-disorder transition. For low skyrmion densities the peak effect is absent since the system is always in a disordered state. We map the dynamical phase transition as a function of temperature, density, drive, and materials parameters, and show that the signatures are similar to those of the superconducting peak effect. Our results are consistent with recent experiments.

DOI: [10.1103/PhysRevB.108.014428](https://doi.org/10.1103/PhysRevB.108.014428)**I. INTRODUCTION**

Skyrmions are particlelike magnetic textures that can form in chiral magnets [1–4]. They have been attracting growing attention as an increasing number of materials are being found that support skyrmions, and a variety of possible applications have been proposed for using skyrmions for memory and novel computing [5,6]. Skyrmions have many similarities to vortices in type-II superconductors [7], including the fact that they have repulsive pairwise interactions [8,9], form triangular lattices [1–3], can be set into motion with an applied current [3,4,10–12], and can interact with and be pinned by quenched disorder so that there is a critical driving force required to set them in motion [10,12–17]. In many skyrmion systems, thermal fluctuations are also relevant, and skyrmions have been shown to exhibit diffusion [18,19], creep behavior [8,16,20–22], skyrmion lattice melting [23,24], and skyrmion glass phases [25]. An important difference between skyrmions and superconducting vortices is that the skyrmions have a strong gyrotropic component to their dynamics due to the Magnus force, which causes the skyrmions to move at an angle with respect to an applied driving force [3,4,8,12,13,15,16,22,26–28]. This gyrotropic term also strongly affects how skyrmions interact with pinning [13,15,16].

One of the most interesting effects observed for superconducting vortex systems is the peak effect, in which the critical depinning force is nonmonotonic and passes through a peak with increasing magnetic field [29–34]. Here, the depinning threshold initially decreases with increasing field as the vortex density increases since the vortex lattice is becoming stiffer; however, just below the upper magnetic field H_{c2} above which superconductivity is destroyed, the depinning threshold shows a rapid increase followed by a downward plunge, leading to a peak in the depinning force [29–32]. It was argued that the

pairwise vortex-vortex interactions are modified and reduced at high fields, leading to a softening of the vortex lattice and a reduction of its shear modulus [30]. A softer lattice can more readily adapt to a random pinning landscape and is better pinned than a stiff lattice. The velocity-force curves also change shape across the peak effect [32], producing a crossing of the curves in which the depinning threshold is lowest above the peak effect but the flow velocity is lowest below the peak effect [35]. The vortex peak effect also occurs for fixed vortex density as a function of increasing temperature [33,36–40]. Again this is counterintuitive since in general for a particle-based system coupled to quenched disorder, an increase in thermal fluctuations should cause the particles to jump more readily out of the wells, resulting in a monotonic decrease of the critical depinning force F_c with increasing temperature T [41,42]. In the vortex case, the vortex-vortex interactions are also modified by the temperature, leading to a softening of the vortex lattice with increasing temperature.

It has been argued that the superconducting peak effect is produced by a transition from an ordered lattice to a disordered phase that occurs when the vortex lattice becomes soft enough for topological defects to proliferate due to the pinning, strongly reducing or breaking down the elasticity of the lattice [32]. In this sense, the peak effect can also be viewed as a melting transition in the presence of quenched disorder [33,34]. Neutron scattering [37,43] and imaging experiments [38,44] have shown transitions from an ordered vortex state below the peak effect to disordered structures at and above the peak effect. In the thermal peak effect, as T is further increased above the peak, F_c decreases again due to increasing thermal hopping in the disordered state. The thermal peak effect can be regarded as resulting from a competition between the reduction of the depinning threshold by increasing temperature and the reduction of the pairwise vortex-vortex interactions that tends to increase the

depinning force. The sudden increase in the critical force then corresponds to a transition from ordered elastic depinning to disordered plastic depinning. Such a change from elastic to plastic depinning will also alter the shape of the velocity-force curves, which have the form $v = (F_D - F_C)^\beta$ with $\beta < 1.0$ in the elastic depinning regime and $\beta > 1.0$ in the plastic depinning regime [42].

Noise fluctuations can also be used to probe the peak effect. An ordered lattice moves with low noise, but near the peak effect the vortex lattice breaks apart and depins plastically, producing large noise, while above the peak the flow becomes more fluidlike and the noise is low again [45]. Since the peak effect separates two different phases, various memory and metastable effects occur when there is a coexistence of the ordered and disordered phases [36,46,47]. Another observation is that the peak effect does not occur in strongly pinned samples where the vortices are always in a disordered state [34]. In general, for systems with weaker pinning the peak effect occurs at higher temperatures, indicating that as the pinning strength decreases, the lattice must be softer in order to permit the order to disorder transition to occur [34]. There can also be a jump up in the critical depinning force at low fields as the vortex density is decreased, which occurs when the vortices become so far apart that the vortex lattice shear modulus drops to a low value and the system becomes disordered [48]. Simulations with modifications to the vortex-vortex interactions have produced a peak in the depinning force [49].

An open question is whether a skyrmion lattice can also show a peak effect phenomenon similar to that found in the superconducting system, and whether there would be similar changes in the transport properties across the order to disorder transition. Recently Wang *et al.* [50] numerically studied the interactions $U(T)$ between two skyrmions as a function of temperature and found that the interactions decrease approximately exponentially with increasing temperature. They proposed that the functional form $U(T) \propto \exp(-T/\lambda^*)$, where λ^* is a material parameter, could be used to introduce temperature dependence of the interaction into a particle-based model of skyrmions. An interaction of this type suggests that if a skyrmion lattice is in the presence of pinning, under increasing temperature the interactions sharply decrease and the lattice softens, making it possible for a transition to occur from an ordered to a disordered lattice.

Interestingly, in the literature [10] it was found that the depinning threshold for skyrmions in MnSi increases with temperature, consistent with the idea that the skyrmion lattice has softened and become better pinned. Luo *et al.* [21] used ultrasound spectroscopy to examine a skyrmion lattice in MnSi and measure the depinning force. They found a regime where the critical depinning current decreases with increasing T followed by an upturn for further increases in T that is correlated with a softening of the skyrmion lattice. This was interpreted as evidence for a skyrmion peak effect similar to that found in the superconducting vortex systems.

In this work we consider a particle-based model for skyrmions interacting with pinning where we add thermal fluctuations and modify the skyrmion pairwise interactions according to the exponential decrease with T proposed by Wang *et al.* [50]. We focus on parameters where the skyrmions

form a lattice that depins elastically at $T = 0$. As the temperature increases, we find that the depinning threshold initially decreases due to increased creep; however, when the pairwise interactions become weak enough, the skyrmion lattice disorders and there is a pronounced increase in the depinning threshold. As the temperature is further increased, the depinning threshold decreases again due to increased thermal hopping and eventually goes to zero when the skyrmions form a liquid. The result is the appearance of a peak effect in the depinning force similar to that found for superconducting vortices. At low skyrmion densities or in regimes where the skyrmions are always disordered even for $T = 0$, there is no peak effect. We also find that the velocity-force curves change concavity across the peak effect, resulting in a crossing of the curves. Above the peak effect temperature T_p where the depinning threshold is low, the velocity in the flow regime is lower than that found for the same drive in the lower temperature elastic system. We also show that the skyrmion Hall angle is nonmonotonic and changes across the peak effect regime. Under an increasing external drive at temperatures above T_p but below the melting temperature T_m , the system can undergo dynamical reordering similar to that found for superconducting vortices [32]. The drive at which reordering occurs diverges as T_m is approached, in agreement with the predictions of Koshelev and Vinokur for driven superconducting vortices [51]. We construct a dynamic phase diagram and show that it is similar to the diagram observed for superconducting vortices [32,52], with pinned lattice, pinned glass, plastic flow, and moving crystal regimes. For constant drive well above the depinning threshold, we find that as the temperature increases, the velocity and skyrmion Hall angle both drop across the elastic to plastic phase transition, but increase at higher temperature and saturate above T_m to the values expected for a pin-free system. Our results could be tested with transport, imaging, neutron scattering, and noise measurements in skyrmion samples that show a lattice regime.

II. SIMULATION

We work with a particle-based model for skyrmions employing a modified Thiele equation approach that has been used in previous studies of skyrmion ordering, depinning, transport, and thermal effects [8,13,16,20,53–55]. We consider a two-dimensional (2D) system of size $L \times L$ with periodic boundary conditions in the x and y directions containing N_s skyrmions and N_p pinning sites. The equation of motion for a single skyrmion i is

$$\alpha_d \mathbf{v}_i + \alpha_m \hat{z} \times \mathbf{v}_i = \mathbf{F}_i^{ss} + \mathbf{F}_i^{sp} + \mathbf{F}^D + \mathbf{F}^T. \quad (1)$$

The skyrmion velocity is $\mathbf{v}_i = d\mathbf{r}_i/dt$ and α_d is the damping term that aligns the skyrmion velocity in the direction of drive. There is also a gyrotropic or Magnus force component, with coefficient α_m , that generates a velocity perpendicular to the net forces acting on the skyrmion. The repulsive skyrmion-skyrmion interaction force is $\mathbf{F}_i^{ss} = \sum_{j=1}^{N_s} A_s K_1(r_{ij}) \hat{\mathbf{r}}_{ij}$, where $r_{ij} = |\mathbf{r}_i - \mathbf{r}_j|$ is the distance between skyrmions i and j and $\hat{\mathbf{r}}_{ij} = (\mathbf{r}_i - \mathbf{r}_j)/r_{ij}$. The coefficient A_s is material dependent. The first-order Bessel function form $K_1(r)$ of the interaction was obtained from a fit to a continuum model [8], and it decreases exponentially at longer range. Imaging studies

have found similar skyrmion interactions that decay exponentially at longer range [56]. The pinning force $\mathbf{F}_i^{sp} = \sum_{k=1}^{N_p} (F_p/r_p)\Theta(r_{ik}^{(p)} - r_p)\hat{\mathbf{r}}_{ik}$ arises from nonoverlapping attractive parabolic wells of maximum range r_p and maximum strength F_p , where $r_{ik}^{(p)} = |\mathbf{r}_i - \mathbf{r}_k^{(p)}|$ is the distance between skyrmion i and pin k and $\hat{\mathbf{r}}_{ik}^{(p)} = (\mathbf{r}_i - \mathbf{r}_k^{(p)})/r_{ik}^{(p)}$. This is the same form of substrate used in previous particle-based models to study skyrmion depinning [13,16]. The driving force $\mathbf{F}^D = F_D\hat{\mathbf{x}}$ is produced by an applied spin-polarized current. The thermal term \mathbf{F}^T is modeled by Langevin kicks with the properties $\langle F^T \rangle = 0$ and $\langle F_i^T(t)F_j^T(t') \rangle = 2\alpha_d k_B T \delta_{ij} \delta(t - t')$.

In the absence of interactions with other skyrmions or pinning sites, a skyrmion moves at an intrinsic Hall angle of $\theta_{sk}^{\text{int}} = \arctan(\alpha_m/\alpha_d)$ with respect to the applied driving force. In the overdamped case, $\theta_{sk}^{\text{int}} = 0^\circ$. We take $\alpha_d^2 + \alpha_m^2 = 1.0$, and throughout this work we fix $\alpha_d = 0.866$ and $\alpha_m = 0.5$, giving an intrinsic skyrmion Hall angle of $\theta_{sk}^{\text{int}} = -30^\circ$ that is well within the range of experimental values. We measure the average skyrmion velocity both parallel, $\langle V_{\parallel} \rangle = \langle N_s^{-1} \sum_i \mathbf{v}_i \cdot \hat{\mathbf{x}} \rangle$, and perpendicular, $\langle V_{\perp} \rangle = \langle N_s^{-1} \sum_i \mathbf{v}_i \cdot \hat{\mathbf{y}} \rangle$, to the applied drive, where each quantity is averaged over 1×10^5 simulation time steps. From these measurements we obtain the observed skyrmion Hall angle $\theta_{sk} = \arctan(\langle V_{\perp} \rangle / \langle V_{\parallel} \rangle)$, which is affected by interactions with the pinning landscape, as shown in both simulation and experiment, and generally increases with increasing drive before saturating to the clean value at high drives well above depinning [13,16,26–28].

Wang *et al.* [50] proposed that the strength $U(T)$ of the pairwise skyrmion-skyrmion interactions decreases exponentially with temperature according to the approximate form $U(T) \propto \exp(-T/\lambda^*)$, where λ^* is a material parameter. Here we consider the interaction of two thermal effects. As the temperature T increases, the magnitude F^T of the thermal fluctuations also increases, which increases the diffusion of the skyrmions. At the same time, the skyrmion-skyrmion interaction coefficient varies as $A_s = A_s^0 \exp(-\kappa T)$, causing the skyrmion lattice to soften with increasing temperature. The model of Wang *et al.* was proposed for pairwise interactions between isolated skyrmions, but we expect that the general form and temperature dependence of the interaction would remain the same for multiple interacting skyrmions forming a lattice in the regime where the particle-based approach can be applied. We focus on a system of size $L = 36$ with $r_p = 0.25$, $N_s = 450$, a skyrmion density of $n_s = 0.4$, $N_p = 672$, a pinning density of $n_p = 0.6$, $F_p = 0.1$, $A_s^0 = 3.0$, and $\kappa = 2.0$, but in later sections of the paper we also consider different skyrmion densities and vary κ over the range $\kappa = 0-3.0$.

III. RESULTS

We first consider the effects on the depinning behavior of independently varying the thermal fluctuations and the skyrmion-skyrmion interactions. We focus on a system with skyrmion density $n_s = 0.4$, $F_p = 0.1$, and $A_s = A_s^0$. For these parameters, at zero temperature the skyrmions form a triangular lattice that depins elastically without the generation of topological defects.

In Fig. 1(a) we plot the velocity-force curves $\langle V_{\parallel} \rangle$ versus F_D for temperatures of $T = 0, 0.1, 0.2, 0.6$, and 1.4 . Here the

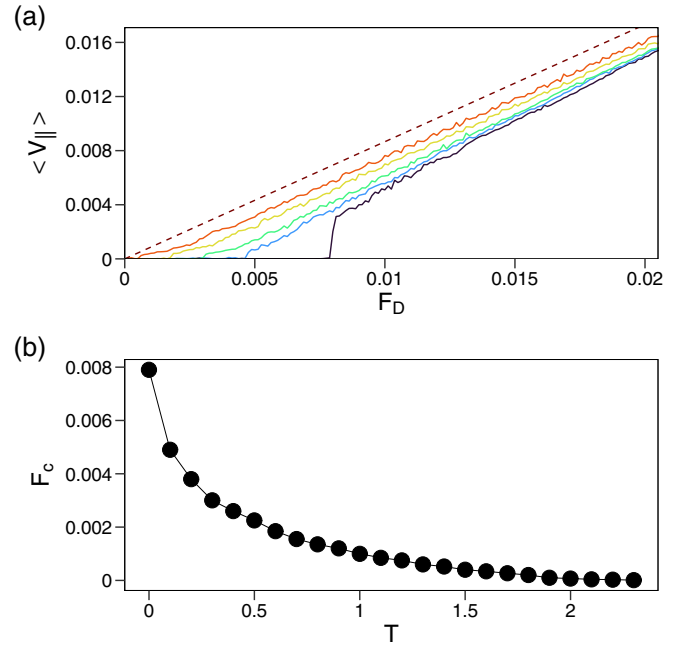


FIG. 1. (a) The skyrmion velocity $\langle V_{\parallel} \rangle$ in the direction of the applied drive vs F_D in a system with fixed skyrmion-skyrmion interaction strength $A_s = A_s^0$ at temperatures $T = 0, 0.1, 0.2, 0.6$, and 1.4 , from bottom to top. The dashed line is the expected response in the absence of pinning. (b) The critical depinning force F_c vs T for the system in (a). The depinning threshold decreases monotonically with increasing T .

skyrmion-skyrmion interaction is not modified as T increases; only the magnitude of the thermal fluctuations increases. The dashed line shows the expected response in a pin-free sample with $F_p = 0$. We find that the depinning threshold decreases monotonically with increasing T , and above depinning, $\langle V_{\parallel} \rangle$ for a fixed value of F_D also decreases monotonically. Figure 1(b) shows that the critical depinning force F_c decreases with increasing T and drops to zero for $T > 2.0$, well below the thermally induced melting temperature of $T_m = 3.0$. The critical force obtained from the perpendicular velocity $\langle V_{\perp} \rangle$ (not shown) exhibits similar behavior, and the drive-dependent skyrmion Hall angle saturates at higher drives as discussed in previous work [20].

Next we introduce thermal modification of the skyrmion-skyrmion interactions but eliminate the thermal fluctuations so that the Langevin kicks have a temperature of $T = 0$. In Fig. 2 we show some representative velocity-force curves for decreasing values of $A_s = 6.0, 3.0, 1.75, 1.5, 1.25, 1.0, 0.75$, and 0.5 . The depinning force F_c increases monotonically with decreasing A_s due to the softening of the skyrmion-skyrmion interactions. For $A_s = 6.0, 3.0, 1.75$, and 1.5 , the depinning transition is elastic and the skyrmions maintain the same neighbors as they depin, while for $A_s = 1.25, 1.0, 0.75$, and 0.5 , the depinning is plastic and the skyrmion lattice breaks apart into riverlike regions of flow. We also find that the shape of the velocity-force curves changes across the transition from elastic to plastic depinning.

In Fig. 3(a) we plot F_c versus A_s for the $T = 0$ samples from Fig. 2, while Fig. 3(b) shows the corresponding

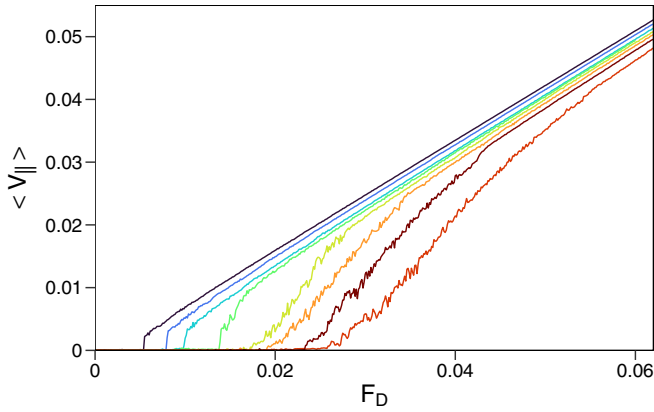


FIG. 2. $\langle V_{\parallel} \rangle$ vs F_D for the system in Fig. 1 at $T = 0$ for modified skyrmion-skyrmion interaction strengths of $A_s = 6.0, 3.0, 1.75, 1.5, 1.25, 1.0, 0.75,$ and 0.5 , from top to bottom. The depinning threshold monotonically increases with decreasing A_s . The depinning transition is elastic for $A_s > 1.25$ and plastic for $A_s \leq 1.25$.

fraction P_6 of sixfold-coordinated skyrmions versus A_s . Here $P_6 = N_s^{-1} \sum_i \delta(z_i - 6)$, where z_i is the coordination number of skyrmion i obtained from a Voronoi construction. For $A_s > 1.25$, $P_6 \approx 1.0$, the depinning is elastic, and F_c decreases slowly with increasing A_s . For $A_s \leq 1.25$, P_6 drops with decreasing A_s as the system becomes disordered, and there is a relatively rapid increase in F_c since the disordered skyrmion lattice is better pinned. As A_s decreases further, F_c continues to increase, and the maximum critical force of $F_c/F_p = 1.0$ occurs when $A_s = 0$ (not shown). The onset of plastic depinning with decreasing A_s can be viewed as representing the first part

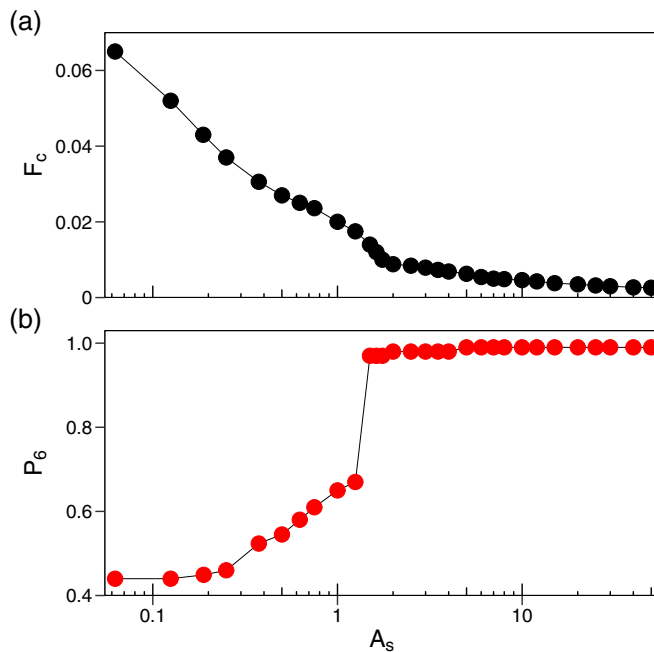


FIG. 3. (a) F_c vs A_s for the system in Fig. 2 with $T = 0$. (b) The corresponding fraction P_6 of sixfold-coordinated skyrmions vs A_s . As A_s decreases, F_c increases, with a more rapid increase appearing at the order to disorder transition near $A_s = 1.25$.

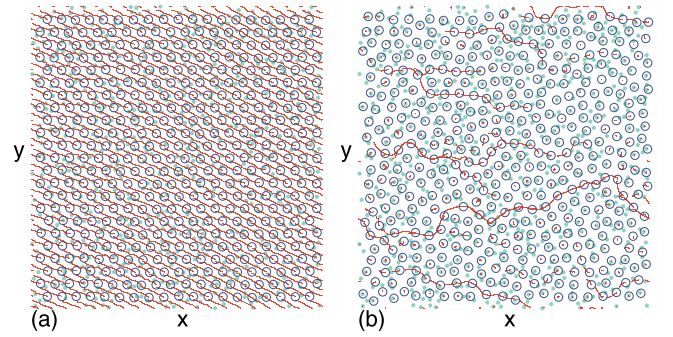


FIG. 4. The pinning site locations (filled circles), skyrmion locations (open circles), and trajectories (lines) for the system in Fig. 3 with $T = 0$. (a) At $A_s = 3.0$ just above depinning, the flow is elastic. (b) At $A_s = 0.5$, the skyrmions are disordered and the depinning is plastic.

of the peak effect in which the topologically disordered lattice softens and can be better pinned than a clean elastic lattice. As A_s decreases further, however, F_c continues to grow, and at $A_s = 0$, $F_c = F_p$, so there is no peak in F_c at nonzero values of A_s .

In Fig. 4(a) we illustrate the pinning site locations and skyrmion positions and trajectories for the system in Fig. 3 at $A_s = 3.0$ just above depinning, where the skyrmions form a lattice that moves as a rigid object. It is also clear that the motion occurs at an angle to the applied drive that is associated with the skyrmion Hall angle. Figure 4(b) shows the same system at $A_s = 0.5$ where the skyrmions are disordered and only some of the skyrmions are moving while the rest of the skyrmions remain pinned. These results show that in the absence of thermal fluctuations, softening the skyrmion lattice increases the depinning threshold, with a rapid increase in the critical force F_c at the order to disorder transition. This suggests that if thermal fluctuations are combined with a weakening of the skyrmion-skyrmion interaction as temperature increases, the two effects will compete, resulting in the emergence of a peak effect in the depinning threshold.

IV. THERMAL MODIFICATION OF THE SKYRMION-SKYRMION INTERACTION

We next consider the case where thermal fluctuations are increased at the same time that the skyrmion-skyrmion interaction is adjusted for temperature using the exponential dependence proposed by Wang *et al.* [50], $A_s = A_s^0 \exp(-\kappa T)$. We fix $\kappa = 2.0$ and set $A_s^0 = 3.0$, so that at $T = 0$ the system forms a triangular solid that depins elastically, as shown in Fig. 3. For these parameters, in a pin-free system with $F_p = 0$, a melting transition occurs at $T_m = 1.125$ via the proliferation of topological defects.

In Fig. 5(a) we plot $\langle V_{\parallel} \rangle$ versus F_D for $T/T_m = 0, 0.26, 0.4346, 0.6086, 0.869, 1.3043,$ and 1.739 , while Fig. 5(b) shows the corresponding skyrmion Hall angle θ_{sk} versus F_D . The system depins elastically for $T/T_m = 0$ and $T/T_m = 0.2$, and in this regime the depinning force decreases with increasing T/T_m . The shape of the velocity-force curve changes for $T/T_m = 0.4346$ and the depinning threshold increases since the depinning transition becomes plastic. For even

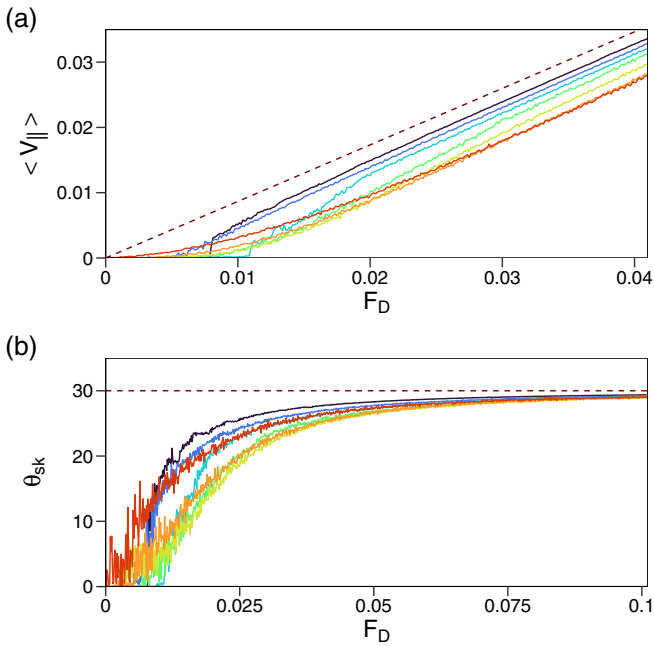


FIG. 5. $\langle V_{\parallel} \rangle$ vs F_D for a system in which we simultaneously increase T while modifying the skyrmion-skyrmion interaction A_s with temperature according to the relation proposed by Wang *et al.* [50]. From top right to bottom right, $T/T_m = 0, 0.26, 0.4346, 0.6086, 0.869, 1.3043, \text{ and } 1.739$, where T_m is the temperature at which a pin-free system with $F_p = 0$ melts. The depinning threshold initially decreases with increasing temperature, increases again to reach its maximum value near $T/T_m = 0.5$, and then decreases again for high T/T_m . We also find a crossing of the velocity-force curves. (b) The corresponding skyrmion Hall angle θ_{sk} vs F_D . Dashed lines indicate the expected response in the absence of pinning.

higher T/T_m , there is an increasing amount of creep in which the velocity becomes finite at lower F_D . A crossing of the velocity-force curves occurs in Fig. 5 since the velocities at higher F_D are lower for higher values of $T/T_m > 0.4346$ compared to $T/T_m < 0.4346$, even though the depinning threshold for $T/T_m > 0.4346$ is lower than that found for $T/T_m < 0.4346$. In the elastic depinning regime for $T/T_m < 0.4346$, θ_{sk} becomes finite just above depinning, and it initially has a low value but increases rapidly with increasing F_D . The steps that appear in the velocity at depinning when $T/T_m = 0$ are caused by an alignment of the angle of skyrmion motion with the symmetry direction of the triangular pinning lattice, an effect that was predicted to lead to steps in the velocity-force curves [57]. This directional locking was studied previously for skyrmions [58]. In the plastic depinning regime, the skyrmion Hall angle is generally lower. The fluctuations of θ_{sk} are largest just above depinning since the angle is calculated from a ratio of two velocities. Figure 5(b) indicates that the skyrmion Hall angle is also nonmonotonic as a function of temperature. The lowest value of θ_{sk} appears for $T/T_m = 1.0$, and there is a crossing of the skyrmion Hall angle curves that is similar to the crossing of the velocity-force curves. The behavior of the skyrmion Hall angle through the peak effect region is discussed in greater detail in Sec. V.

From the velocity-force curves, we obtain the depinning force F_c , defined as the value of F_D at which we first observe

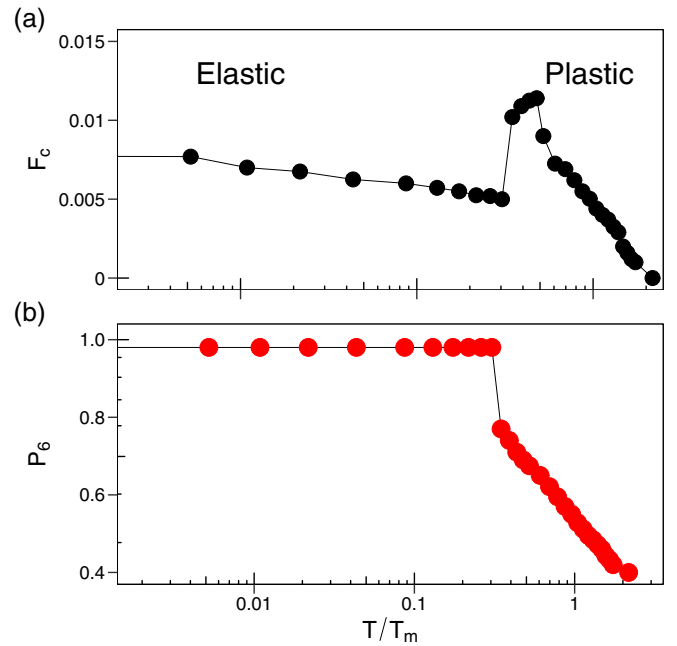


FIG. 6. (a) F_c vs T/T_m obtained from the velocity-force curves for the system in Fig. 5. (b) The corresponding P_6 vs T/T_m , showing that the increase in F_c is associated with a disordering transition.

$\langle V_{\parallel} \rangle > 0.001$. In Fig. 6 we plot F_c and P_6 at depinning versus T/T_m , where T_m is the temperature at which the $F_p = 0$ system melts. Here, F_c initially drops with increasing T/T_m while P_6 remains close to 1, indicating that elastic depinning is occurring. For temperatures above $T/T_m = 0.4346$, there is a proliferation of topological defects and F_c first increases with temperature before decreasing due to enhanced thermal hopping.

The overall behavior of F_c shown in Fig. 6 is very similar to that found for the thermal peak effect in type-II superconductors, where there is a jump up in the critical depinning force at the elastic to plastic or order to disorder transition, coinciding with a change in the shape of the velocity-force curves that causes a crossing of the curves [33,35–40,49]. Figure 6 also illustrates that the disordering transition occurs at $T/T_m < 1.0$, similar to the peak effect in superconductors where the combination of thermal fluctuations and pinning cause the vortex lattice to disorder at temperatures below the clean melting temperature. In general, for the superconducting system, as F_p increases, the temperature T_p at which the peak effect occurs is reduced.

V. DYNAMIC ORDERING

In superconducting vortex systems, Wigner crystals, and skyrmions, it was shown that when the system is in a plastic depinning regime, as the drive increases the effect of the pinning on the moving particles is reduced and the system can dynamically order into a moving crystal or moving smectic with few topological defects at high drives [16,32,42,58–63]. In Ref. [32], Higgins and Bhattacharya construct a dynamic phase diagram across the peak effect showing a transition in the flow above depinning from elastic to disordered, where in

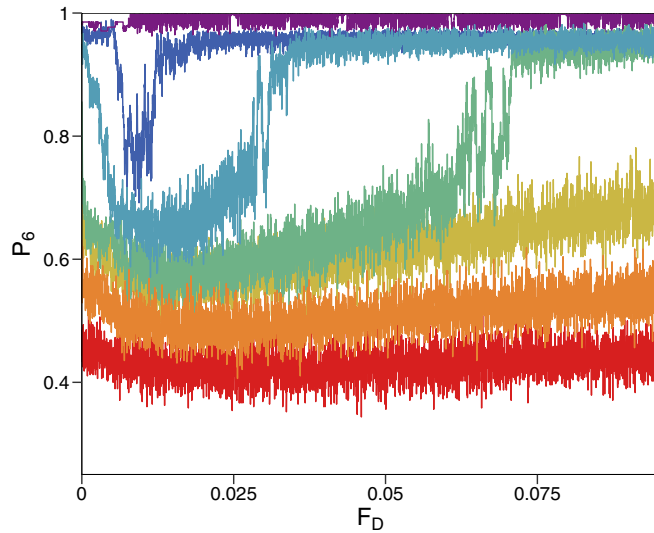


FIG. 7. P_6 vs F_D for the system in Fig. 5 for $T/T_m = 0.174, 0.348, 0.608, 0.869, 1.087, 1.304, \text{ and } 1.74$, from top to bottom. For $T/T_m < 1.0$, the system dynamically orders into a moving crystal at higher drives.

the disordered regime above the peak effect, for higher drives the flow becomes ordered again. Koshelev and Vinokur [51] then performed simulations of the plastic depinning of vortices, and found that at higher drives when the vortices are moving sufficiently rapidly over the pinning, the vortex lattice can dynamically reform. The drive at which this dynamical ordering occurs diverges near the melting temperature of the pin-free system.

We next study whether dynamical reordering also occurs across the skyrmion peak effect with characteristics that are similar to what is found for the dynamical ordering across the peak effect in the superconducting case [32,51]. In Fig. 7 we plot P_6 versus F_D for the system in Figs. 5 and 6 at $T/T_m = 0.174, 0.348, 0.608, 0.869, 1.087, 1.304, \text{ and } 1.74$. At $T/T_m = 0.174$, the system is always in an ordered state and $P_6 \approx 1$ at all drives, while for $T/T_m = 0.348, 0.608, \text{ and } 0.869$, the system is disordered at depinning but at high drive undergoes a dynamical reordering transition in which P_6 increases to a value close to $P_6 = 0.95$. The drive at which the dynamical ordering occurs increases with increasing T/T_m , and for $T/T_m > 1.0$, the system remains disordered for all values of F_D .

From the features of the F_c and P_6 curves, we construct a dynamical phase diagram as a function of F_D versus T/T_m , as shown in Fig. 8. There is a pinned skyrmion crystal that depins elastically to a moving crystal as well as a pinned glass that depins plastically to a moving fluid state. Above the peak effect regime, there is a transition from a moving fluid into a moving crystal with increasing drive, and the value of F_D at which this dynamic reordering occurs diverges as $T/T_m = 1.0$ is approached. For sufficiently high temperatures, the pinned phase is lost and the system is permanently in the moving fluid state. The overall shape of the phase diagram is very similar to that of the superconducting peak effect dynamical phase diagram obtained experimentally by Bhattacharya and Higgins [32], while the divergence in the reordering driving

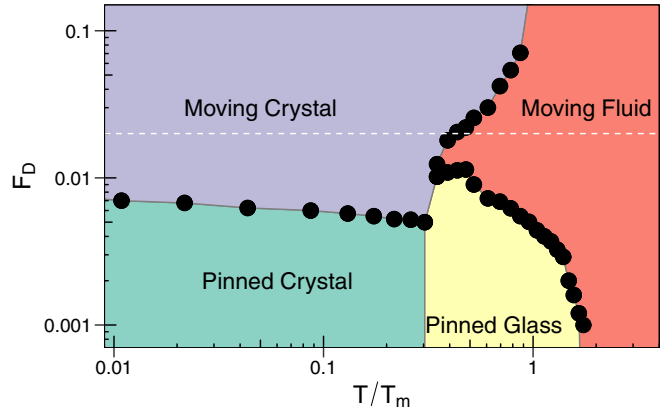


FIG. 8. Dynamic phase diagram as a function of F_D vs T/T_m constructed from the velocity-force curves and P_6 data in Figs. 6 and 8 showing a pinned crystal, moving crystal, pinned glass, and moving glass. The horizontal dashed line indicates the value of F_D at which the velocity and skyrmion Hall angle data in Fig. 9 were obtained.

force upon approaching $T/T_m = 1$ agrees with the simulation results of Koshelev and Vinokur [51]. We note that there could be additional phases beyond those shown in Fig. 8. For example, the moving crystal could also contain regions of a moving smectic phase, and it could be possible to draw a distinction between a moving glass and a moving liquid.

In the superconducting system, consequences of the peak effect appear even for drives well above depinning. For example, it is possible to apply a constant current with $F_D > F_c$ while increasing the temperature, as indicated by the horizontal dashed line at $F_D = 0.2$ in Fig. 8. Here, the velocity parallel to the drive exhibits a drop at the temperature corresponding to the elastic to plastic transition, as shown in Fig. 9(a) where there is a minimum in $\langle V_{\parallel} \rangle$ close to $T/T_m = 1.0$. A similar dip appears in the perpendicular velocity and the absolute velocity. As shown in Fig. 9(b), there is a corresponding drop in the magnitude of the skyrmion Hall angle. For higher T/T_m , $|\theta_{sk}|$ approaches the clean limit value expected in a sample with $F_p = 0$. The increase in skyrmion Hall angle in the fluid state results because individual skyrmions interact less strongly with the pinning sites and therefore undergo less deflection upon passing through a pinning site, bringing $|\theta_{sk}|$ closer to the value it would have in the absence of pinning. The magnitude of the drop in P_6 diminishes with increasing F_D .

In Fig. 10 we show a heat map of the skyrmion Hall angle as a function of F_D versus T/T_m . For a fixed value of F_D , θ_{sk} increases as the temperature passes through the transition from elastic to plastic behavior. The skyrmion Hall angle always increases with increasing F_D , and there is also an increase in θ_{sk} with increasing temperature for the highest values of T/T_m .

In Fig. 11(a) we plot the skyrmion locations and trajectories along with the pinning site locations for the system in Fig. 9 at $F_D = 0.02$ and $T/T_m = 0.28$ in the elastic regime. The skyrmions exhibit some random motion due to the thermal fluctuations, but form a triangular lattice that moves as a rigid body at an angle to the applied drive. At $T/T_m = 1.74$, Fig. 11(b) indicates that the same system is disordered and

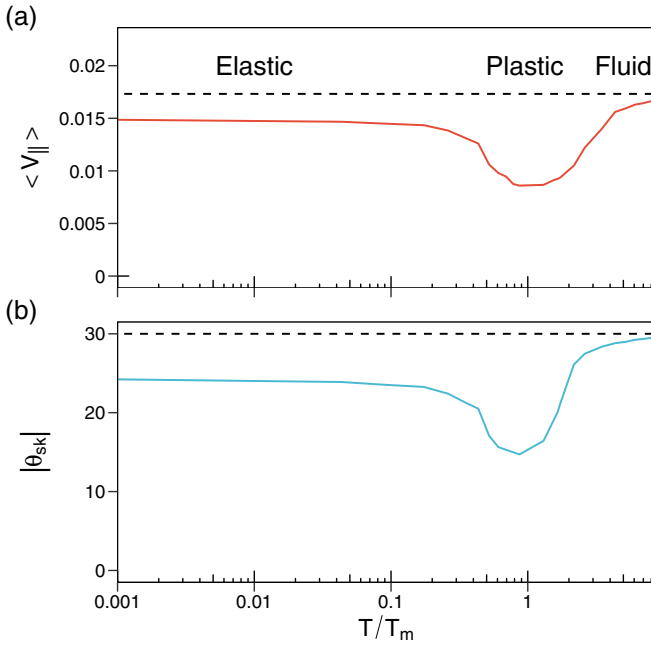


FIG. 9. (a) $\langle V_{\parallel} \rangle$ vs T/T_m for a slice at $F_D = 0.02$, above the depinning force, from the phase diagram in Fig. 8. There is a dip across the order to disorder transition. (b) The corresponding skyrmion Hall angle $|\theta_{sk}|$ vs T/T_m , which also shows a dip. For $T/T_m > 1.0$, the values of both quantities approach the $F_p = 0$ values (dashed lines).

contains regions of flowing skyrmions coexisting with pinned regions. Due to the significant amount of thermal hopping, finite skyrmion velocities extend down to much lower values of F_D compared to the $T/T_m = 0.28$ sample. At low drives in

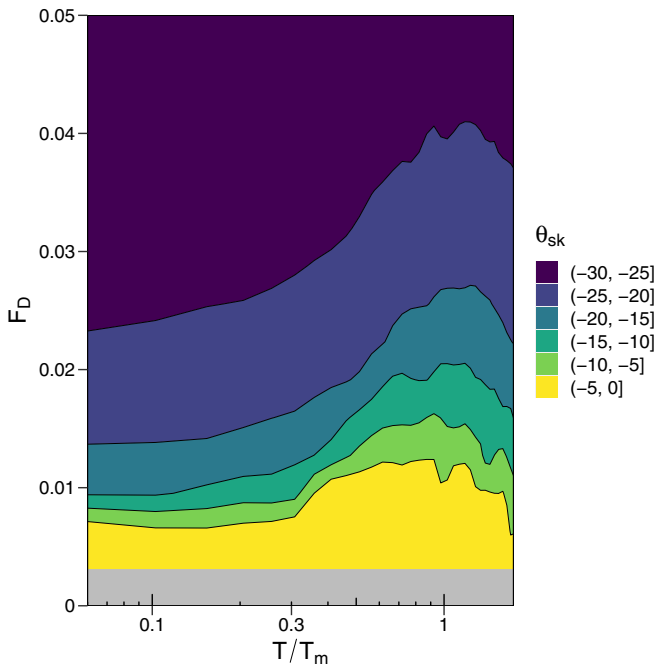


FIG. 10. Heat map of the skyrmion Hall angle θ_{sk} in degrees as a function of F_D vs T/T_m . In the gray region, the skyrmions are not flowing steadily and θ_{sk} is undefined.

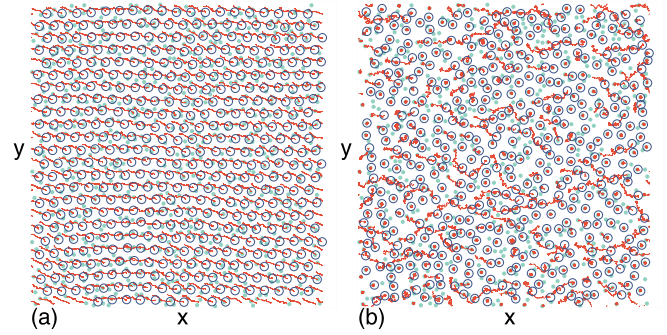


FIG. 11. The pinning site locations (filled circles), skyrmion locations (open circles), and trajectories (lines) for the system in Fig. 8 at $F_D = 0.02$. (a) $T/T_m = 0.28$ where the flow is elastic. (b) $T/T_m = 1.74$ where the flow is fluid.

the elastic depinning regime, the creep motion must occur in a correlated fashion since plastic distortions of the skyrmion lattice are suppressed. As a result, for $F_D = 0.02$ and $T/T_m = 0.28$, all of the skyrmions move at the same velocity, while for the same drive at $T/T_m = 1.74$, due to the thermally induced breakdown of the lattice structure, some skyrmions remain temporarily pinned while other skyrmions are moving, giving a reduced average velocity. This is what produces the crossing of the velocity-force curves. At even higher temperatures, the hopping becomes so rapid that the average velocity in the liquid phase at $F_D = 0.02$ is higher than the average velocity in the elastic regime, as was shown in Fig. 9.

VI. SKYRMION DENSITY AND MATERIALS PARAMETERS

Since the peak effect is correlated with an order to disorder transition, the next question is whether the peak effect can still occur if the system is always disordered. In the case of a single skyrmion, there should not be a peak effect since collective effects are absent and there can be no disorder to order transition. This suggests that in samples with finite pinning strength, for low skyrmion densities when the skyrmions are sufficiently far apart that skyrmion-skyrmion interactions become unimportant, the skyrmion lattice will always be disordered and the peak effect should be absent. In Fig. 12 we plot the critical depinning force F_c versus T/T_m for skyrmion densities of $n_s = 0.2, 0.3, 0.4, 0.5$, and 0.6 . Up until this point we have focused on samples with $n_s = 0.4$. For $n_s > 0.2$, the skyrmions form a crystal and undergo elastic depinning over an extended range of temperatures, with a peak effect appearing at the order to disorder transition temperature. For $n_s \leq 0.2$, the skyrmions are sufficiently far apart that they are disordered even at $T/T_m = 0$. In this case, the overall value of F_c is much higher, and there is no peak effect. For $n_s \geq 0.2$, as the skyrmion density increases, the peak effect shifts to higher temperatures and the overall effectiveness of the pinning is reduced. This is consistent with observations in superconductors where for cleaner samples the overall pinning of the vortices is reduced and the peak effect occurs at high temperatures, while for samples with strong pinning, the peak effect is lost.

As the skyrmion density increases, there is a more pronounced difference in the shape of the velocity-force curves

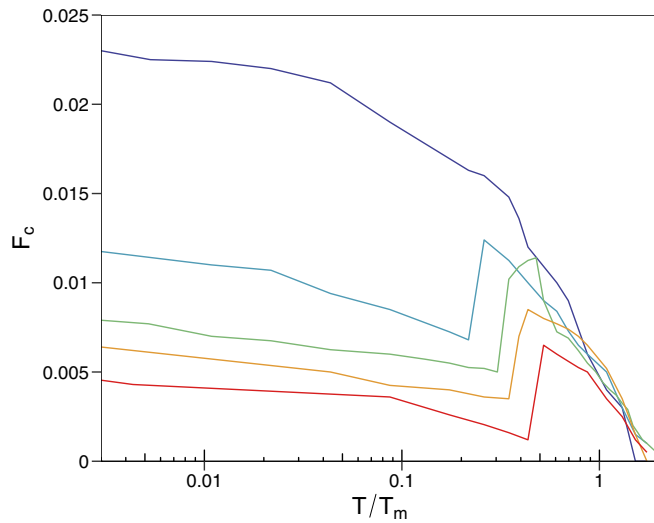


FIG. 12. The critical depinning force F_c vs T/T_m for the system in Fig. 9 at varied skyrmion density $n_s = 0.2, 0.3, 0.4, 0.5$, and 0.6 , from top to bottom. For $n_s = 0.2$, the system is disordered even at $T/T_m = 0$ and there is no peak effect.

on either side of the peak effect, as shown in Fig. 13 where we plot $\langle V_{\parallel} \rangle$ versus F_D for a sample with $n_s = 0.6$ at $T = 0, 0.5, 0.6, 1.5$, and 2.0 . The disordering transition in this case occurs at $T = 0.6$, and the depinning threshold reaches its highest value at this temperature. For higher temperatures, the depinning threshold drops and the velocity-force curves change shape, resulting in a clear crossing of the curves.

Since the temperature dependence of the skyrmion-skyrmion pairwise interaction is given by $\exp(-\kappa T)$ in the model of Wang *et al.* [50], we next consider how the peak effect varies for changing κ . In Fig. 14 we plot F_c versus T/T_m for the $n_s = 0.6$ sample from Fig. 9 at $\kappa = 3, 2, 1, 0.75, 0.5$, and 0 from top to bottom. The peak effect shifts to higher temperatures as κ decreases. Here the curves have been normalized to T_m for the $\kappa = 2.0$ system.

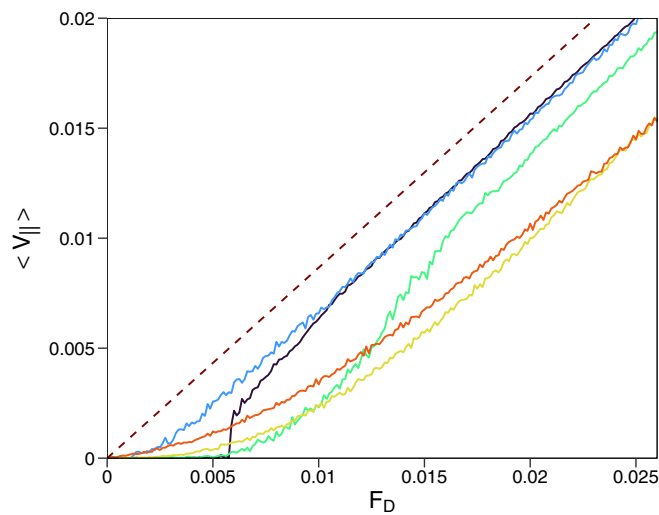


FIG. 13. $\langle V_{\parallel} \rangle$ vs F_D for a sample from Fig. 11 with $n_s = 0.6$ at $T = 0.0$ (black), 0.5 (blue), 0.6 (yellow), 1.5 (green), and 2.0 (orange). There is a clear change in the shape of the velocity-force curves across the peak effect, resulting in a crossing of the velocity-force curves.

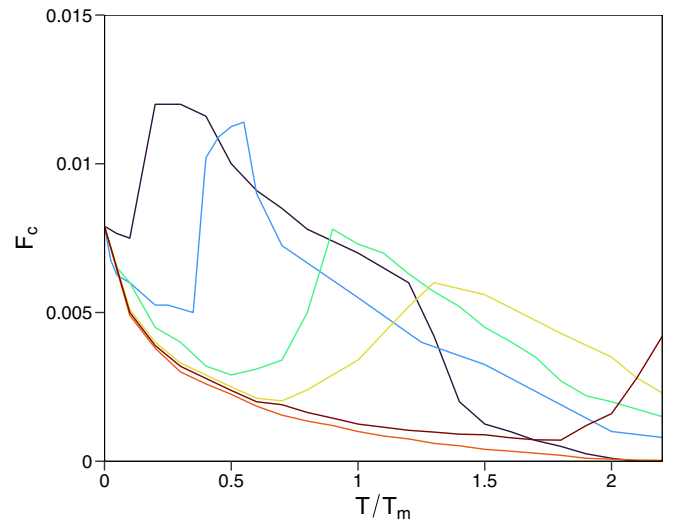


FIG. 14. F_c vs T/T_m for the same system from Fig. 9 with $n_s = 0.4$ at $\kappa = 3, 2, 1, 0.75, 0.5$, and 0 from top to bottom. The peak effect shifts to higher temperatures as κ decreases. Here the curves have been normalized to T_m for the $\kappa = 2.0$ system.

$0.75, 0.5$, and 0 . For $\kappa = 3.0$, the peak effect appears at low temperatures. The $\kappa = 2.0$ system was discussed above, and for $\kappa = 1.0, 0.75$, and 0.5 , the peak effect occurs at higher temperatures while the decrease in F_c with increasing T/T_m becomes more pronounced as κ gets smaller. For $\kappa = 0.0$, there is no peak effect and F_c drops all the way to zero before the system can disorder. In this case, by the time the temperature is high enough to melt the skyrmion lattice, the individual skyrmions are easily able to hop thermally out of the pinning wells. This result indicates that for large κ the system may disorder rapidly with increasing T or always remain disordered, while in samples with small κ , the peak effect will occur at higher temperatures closer to the bulk melting transition. In Fig. 15 we highlight a dynamic phase diagram as a function of T/T_m versus κ showing the order to disorder transition. The transition point should also depend on the strength of the pinning and the skyrmion density.

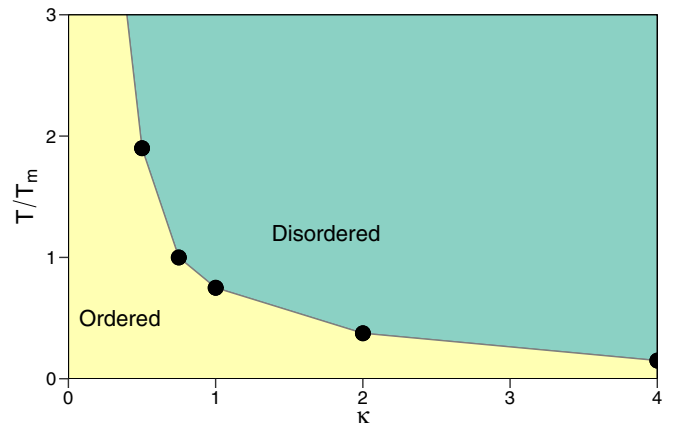


FIG. 15. Dynamic phase diagram of the order to disorder transition as a function of T vs κ for the system in Fig. 13 with $n_s = 0.4$. Here the temperature has been normalized using T_m for the $\kappa = 2.0$ system.

VII. DISCUSSION

An open question is whether a skyrmion peak effect could also occur as a function of applied magnetic field. If the strength of the skyrmion-skyrmion interaction diminishes with increasing field, it could be possible that an order to disorder transition accompanied by a peak effect could occur for increasing magnetic field. In superconducting vortex systems, the number of vortices increases monotonically with magnetic field, so the elastic modulus of the vortex lattice rises with increasing magnetic field, but near the upper critical field H_{c2} , the vortex-vortex interaction strength is reduced when the penetration depth diverges. For skyrmions, the magnetic field dependence is more complex, since not only is the number of skyrmions not a monotonic function of applied magnetic field, but also the size of the skyrmions can change with magnetic field. In principle, a peak effect will occur whenever the skyrmions form an elastic lattice that can transition into a disordered state as a function of applied magnetic field or temperature. There is already some evidence that a skyrmion lattice can thermally melt [24], so it would be interesting to study the transport in these systems while some feature such as skyrmion density or pinning strength is tuned.

In this work, we considered 2D systems; however, many skyrmion systems contain three-dimensional (3D) linelike objects, and a peak effect is known to occur in superconducting vortex systems where the vortices take the form of 3D lines. As long as the strength of the pairwise skyrmion interactions decreases with increasing temperature, there should be a peak effect in a 3D skyrmion system if pinning is present. In fact, it could be possible that the order-disorder transition at the peak effect is second order in 2D systems and first order in 3D systems. If a skyrmion peak effect can occur in 3D samples, it could have a variety of interesting properties such as metastable dynamics. These could appear when the system is prepared in a disordered state under conditions where the steady state is ordered, or vice versa. Metastable behaviors have been observed in superconducting vortices near the peak effect regime [46,64]. We used a particle-based model to explore the skyrmion peak effect; however, it would be interesting to further probe the behavior with a continuum-based model, provided that the system is sufficiently large to exhibit a clear elastic to plastic transition. The continuum model could capture additional effects such as shape distortions of the skyrmions across the peak effect. We also assumed a constant Magnus force; however, if the skyrmions change in size across the peak effect, the Magnus force could be altered.

In our work we assume that the damping constant is fixed; however, in Refs. [65,66], it was noted that changing the skyrmion size can also change the damping. In this work we only consider changing the skyrmion interaction strength as the skyrmion size changes. In general, changing the damping will not change the elastic to plastic phase transition that

occurs across a peak effect, but will instead change the overall velocities. Thus there should still be an observable dip in the velocity across the peak effect, and the velocity should later increase again on the fluid side of the transition.

VIII. SUMMARY

We have numerically investigated a thermal skyrmion peak effect for a skyrmion lattice driven over quenched disorder. As the thermal fluctuations increase, the effectiveness of the pinning is reduced due to thermal hopping, but the strength of the skyrmion-skyrmion interactions is exponentially reduced as proposed by Wang *et al.* [50]. The skyrmion peak effect is similar to the peak effect associated with an order to disorder or elastic to plastic transition in superconducting vortex systems. When the pinning is weak, the skyrmions form a lattice that depins elastically at $T = 0$. As the temperature increases, the depinning threshold decreases, but when the skyrmion-skyrmion interactions become soft enough, there is an order to disorder transition to a skyrmion glass phase accompanied by a large increase in the depinning threshold. As the temperature is further increased, thermal hopping reduces the depinning threshold again, resulting in the appearance of a peak in the depinning force. The peak effect occurs for temperatures below the melting temperature of the skyrmion lattice in the absence of quenched disorder. Across the peak effect, we find a change in the shape of the velocity-force curves and a crossing of the curves similar to what is found for the superconducting peak effect. For a constant drive, even above the depinning threshold the velocity and skyrmion Hall angle both show a drop across the peak effect. We construct a dynamical phase diagram and find that there can be a dynamical reordering transition for increasing drive above the peak effect temperature but below the clean melting temperature. We map the different phases and the nonmonotonic behavior of the skyrmion Hall angle through the peak effect. We show that the peak effect should be robust whenever a skyrmion lattice can form with skyrmion-skyrmion interactions that are modified by temperature. Our results are also consistent with several experimental studies that have shown an increase in the critical current for skyrmion lattices with increasing temperature.

ACKNOWLEDGMENTS

We gratefully acknowledge the support of the U.S. Department of Energy through the LANL/LDRD program for this work. This work was supported by the U.S. Department of Energy through the Los Alamos National Laboratory. Los Alamos National Laboratory is operated by Triad National Security, LLC, for the National Nuclear Security Administration of the U.S. Department of Energy (Contract No. 892333218NCA000001).

-
- [1] S. Mühlbauer, B. Binz, F. Jonietz, C. Pfleiderer, A. Rosch, A. Neubauer, R. Georgii, and P. Böni, Skyrmion lattice in a chiral magnet, *Science* **323**, 915 (2009).
 [2] X. Z. Yu, Y. Onose, N. Kanazawa, J. H. Park, J. H. Han, Y. Matsui, N. Nagaosa, and Y. Tokura, Real-space observation of

a two-dimensional skyrmion crystal, *Nature (London)* **465**, 901 (2010).

- [3] N. Nagaosa and Y. Tokura, Topological properties and dynamics of magnetic skyrmions, *Nat. Nanotechnol.* **8**, 899 (2013).

- [4] K. Everschor-Sitte, J. Masell, R. M. Reeve, and M. Kläui, Perspective: Magnetic skyrmions—Overview of recent progress in an active research field, *J. Appl. Phys.* **124**, 240901 (2018).
- [5] A. Fert, N. Reyren, and V. Cros, Magnetic skyrmions: advances in physics and potential applications, *Nat. Rev. Mater.* **2**, 17031 (2017).
- [6] K. Wang, V. Bheemarasetty, J. Duan, S. Zhou, and G. Xiao, Fundamental physics and applications of skyrmions: A review, *J. Magn. Magn. Mater.* **563**, 169905 (2022).
- [7] G. Blatter, M. V. Feigel'man, V. B. Geshkenbein, A. I. Larkin, and V. M. Vinokur, Vortices in high-temperature superconductors, *Rev. Mod. Phys.* **66**, 1125 (1994).
- [8] S.-Z. Lin, C. Reichhardt, C. D. Batista, and A. Saxena, Particle model for skyrmions in metallic chiral magnets: Dynamics, pinning, and creep, *Phys. Rev. B* **87**, 214419 (2013).
- [9] R. Brearton, G. van der Laan, and T. Hesjedal, Magnetic skyrmion interactions in the micromagnetic framework, *Phys. Rev. B* **101**, 134422 (2020).
- [10] T. Schulz, R. Ritz, A. Bauer, M. Halder, M. Wagner, C. Franz, C. Pfleiderer, K. Everschor, M. Garst, and A. Rosch, Emergent electrodynamics of skyrmions in a chiral magnet, *Nat. Phys.* **8**, 301 (2012).
- [11] X. Z. Yu, N. Kanazawa, W. Z. Zhang, T. Nagai, T. Hara, K. Kimoto, Y. Matsui, Y. Onose, and Y. Tokura, Skyrmion flow near room temperature in an ultralow current density, *Nat. Commun.* **3**, 988 (2012).
- [12] J. Iwasaki, M. Mochizuki, and N. Nagaosa, Universal current-velocity relation of skyrmion motion in chiral magnets, *Nat. Commun.* **4**, 1463 (2013).
- [13] C. Reichhardt, D. Ray, and C. J. Olson Reichhardt, Collective Transport Properties of Driven Skyrmions with Random Disorder, *Phys. Rev. Lett.* **114**, 217202 (2015).
- [14] S. Woo, K. Litzius, B. Krüger, M.-Y. Im, L. Caretta, K. Richter, M. Mann, A. Krone, R. M. Reeve, M. Weigand, P. Agrawal, I. Lemesh, M.-A. Mawass, P. Fischer, M. Kläui, and G. S. D. Beach, Observation of room-temperature magnetic skyrmions and their current-driven dynamics in ultrathin metallic ferromagnets, *Nat. Mater.* **15**, 501 (2016).
- [15] W. Legrand, D. Maccariello, N. Reyren, K. Garcia, C. Moutafis, C. Moreau-Luchaire, S. Coffin, K. Bouzehouane, V. Cros, and A. Fert, Room-temperature current-induced generation and motion of sub-100 nm skyrmions, *Nano Lett.* **17**, 2703 (2017).
- [16] C. Reichhardt, C. J. O. Reichhardt, and M. V. Milošević, Statics and dynamics of skyrmions interacting with disorder and nanostructures, *Rev. Mod. Phys.* **94**, 035005 (2022).
- [17] R. Gruber, J. Zázvorka, M. A. Brems, D. R. Rodrigues, T. Dohi, N. Kerber, B. Seng, M. Vafaee, K. Everschor-Sitte, P. Virnau, and M. Kläui, Skyrmion pinning energetics in thin film systems, *Nat. Commun.* **13**, 3144 (2022).
- [18] J. Zázvorka, F. Jakobs, D. Heinze, N. Keil, S. Kromin, S. Jaiswal, K. Litzius, G. Jakob, P. Virnau, D. Pinna, K. Everschor-Sitte, L. Rózsa, A. Donges, U. Nowak, and M. Kläui, Thermal skyrmion diffusion used in a reshuffler device, *Nat. Nanotechnol.* **14**, 658 (2019).
- [19] L. Zhao, Z. Wang, X. Zhang, X. Liang, J. Xia, K. Wu, H.-A. Zhou, Y. Dong, G. Yu, K. L. Wang, X. Liu, Y. Zhou, and W. Jiang, Topology-Dependent Brownian Gyromotion of a Single Skyrmion, *Phys. Rev. Lett.* **125**, 027206 (2020).
- [20] C. Reichhardt and C. J. O. Reichhardt, Thermal creep and the skyrmion Hall angle in driven skyrmion crystals, *J. Phys.: Condens. Matter* **31**, 07LT01 (2018).
- [21] Y. Luo, S.-Z. Lin, M. Leroux, N. Wakeham, D. M. Fobes, E. D. Bauer, J. B. Betts, J. D. Thompson, A. Migliori, M. Janoschek, and B. Maiorov, Skyrmion lattice creep at ultra-low current densities, *Commun. Mater.* **1**, 83 (2020).
- [22] K. Litzius, J. Leliaert, P. Bassirian, D. Rodrigues, S. Kromin, I. Lemesh, J. Zázvorka, K.-J. Lee, J. Mulkers, N. Kerber, D. Heinze, N. Keil, R. M. Reeve, M. Weigand, B. Van Waeyenberge, G. Schütz, K. Everschor-Sitte, G. S. D. Beach, and M. Kläui, The role of temperature and drive current in skyrmion dynamics, *Nat. Electron.* **3**, 30 (2020).
- [23] P. Huang, T. Schonemberger, M. Cantoni, L. Heinen, A. Magrez, A. Rosch, F. Carbone, and H. M. Rønnow, Melting of a skyrmion lattice to a skyrmion liquid via a hexatic phase, *Nat. Nanotechnol.* **15**, 761 (2020).
- [24] P. Baláz, M. Paściak, and J. Hlinka, Melting of Néel skyrmion lattice, *Phys. Rev. B* **103**, 174411 (2021).
- [25] S. Hoshino and N. Nagaosa, Theory of the magnetic skyrmion glass, *Phys. Rev. B* **97**, 024413 (2018).
- [26] W. Jiang, X. Zhang, G. Yu, W. Zhang, X. Wang, M. B. Jungfleisch, J. E. Pearson, X. Cheng, O. Heinonen, K. L. Wang, Y. Zhou, A. Hoffmann, and S. G. E. te Velthuis, Direct observation of the skyrmion Hall effect, *Nat. Phys.* **13**, 162 (2017).
- [27] K. Litzius, I. Lemesh, B. Krüger, P. Bassirian, L. Caretta, K. Richter, F. Büttner, K. Sato, O. A. Tretiakov, J. Förster, R. M. Reeve, M. Weigand, I. Bykova, H. Stoll, G. Schütz, G. S. D. Beach, and M. Kläui, Skyrmion Hall effect revealed by direct time-resolved X-ray microscopy, *Nat. Phys.* **13**, 170 (2017).
- [28] R. Juge, S.-G. Je, D. S. Chaves, L. D. Buda-Prejbeanu, J. Peña-García, J. Nath, I. M. Miron, K. G. Rana, L. Aballe, M. Foerster, F. Genuzio, T. O. Menteş, A. Locatelli, F. Maccherozzi, S. S. Dhesi, M. Belmeguenai, Y. Roussigné, S. Auffret, S. Pizzini, G. Gaudin *et al.*, Current-Driven Skyrmion Dynamics and Drive-Dependent Skyrmion Hall Effect in an Ultrathin Film, *Phys. Rev. Appl.* **12**, 044007 (2019).
- [29] W. DeSORBO, The peak effect in substitutional and interstitial solid solutions of high-field superconductors, *Rev. Mod. Phys.* **36**, 90 (1964).
- [30] A. B. Pippard, A possible mechanism for peak effect in type II superconductors, *Philos. Mag.* **19**, 217 (1969).
- [31] R. Wördenweber, P. H. Kes, and C. C. Tsuei, Peak and history effects in two-dimensional collective flux pinning, *Phys. Rev. B* **33**, 3172 (1986).
- [32] S. Bhattacharya and M. J. Higgins, Dynamics of a Disordered Flux Line Lattice, *Phys. Rev. Lett.* **70**, 2617 (1993).
- [33] W. K. Kwok, J. A. Fendrich, C. J. van der Beek, and G. W. Crabtree, Peak Effect as a Precursor to Vortex Lattice Melting in Single Crystal $\text{YBa}_2\text{Cu}_3\text{O}_{7-\delta}$, *Phys. Rev. Lett.* **73**, 2614 (1994).
- [34] S. S. Banerjee, S. Ramakrishnan, A. K. Grover, G. Ravikumar, P. K. Mishra, V. C. Sahni, C. V. Tomy, G. Balakrishnan, D. M. Paul, P. L. Gammel, D. J. Bishop, E. Bucher, M. J. Higgins, and S. Bhattacharya, Peak effect, plateau effect, and fishtail anomaly: The reentrant amorphization of vortex matter in 2H-NbSe_2 , *Phys. Rev. B* **62**, 11838 (2000).
- [35] M. J. Higgins and S. Bhattacharya, Varieties of dynamics in a disordered flux-line lattice, *Phys. C: Supercond. Appl.* **257**, 232 (1996).

- [36] Y. Paltiel, E. Zeldov, Y. N. Myasoedov, H. Shtrikman, S. Bhattacharya, M. J. Higgins, Z. L. Xiao, E. Y. Andrei, P. L. Gammel, and D. J. Bishop, Dynamic instabilities and memory effects in vortex matter, *Nature (London)* **403**, 398 (2000).
- [37] X. S. Ling, S. R. Park, B. A. McClain, S. M. Choi, D. C. Dender, and J. W. Lynn, Superheating and Supercooling of Vortex Matter in a Nb Single Crystal: Direct Evidence for a Phase Transition at the Peak Effect from Neutron Diffraction, *Phys. Rev. Lett.* **86**, 712 (2001).
- [38] A. M. Troyanovski, M. van Hecke, N. Saha, J. Aarts, and P. H. Kes, STM Imaging of Flux Line Arrangements in the Peak Effect Regime, *Phys. Rev. Lett.* **89**, 147006 (2002).
- [39] S. Mohan, J. Sinha, S. S. Banerjee, and Y. Myasoedov, Instabilities in the Vortex Matter and the Peak Effect Phenomenon, *Phys. Rev. Lett.* **98**, 027003 (2007).
- [40] R. Toft-Petersen, A. B. Abrahamsen, S. Balog, L. Porcar, and M. Laver, Decomposing the Bragg glass and the peak effect in a type-II superconductor, *Nat. Commun.* **9**, 901 (2018).
- [41] D. S. Fisher, Collective transport in random media: from superconductors to earthquakes, *Phys. Rep.* **301**, 113 (1998).
- [42] C. Reichhardt and C. J. Olson Reichhardt, Depinning and nonequilibrium dynamic phases of particle assemblies driven over random and ordered substrates: a review, *Rep. Prog. Phys.* **80**, 026501 (2017).
- [43] P. L. Gammel, U. Yaron, A. P. Ramirez, D. J. Bishop, A. M. Chang, R. Ruel, L. N. Pfeiffer, E. Bucher, G. D'Anna, D. A. Huse, K. Mortensen, M. R. Eskildsen, and P. H. Kes, Structure and Correlations of the Flux Line Lattice in Crystalline Nb through the Peak Effect, *Phys. Rev. Lett.* **80**, 833 (1998).
- [44] S. C. Ganguli, H. Singh, G. Saraswat, R. Ganguly, V. Bagwe, P. Shirage, A. Thamizhavel, and P. Raychaudhuri, Disordering of the vortex lattice through successive destruction of positional and orientational order in a weakly pinned $\text{Co}_{0.0075}\text{NbSe}_2$ single crystal, *Sci. Rep.* **5**, 10613 (2015).
- [45] A. C. Marley, M. J. Higgins, and S. Bhattacharya, Flux Flow Noise and Dynamical Transitions in a Flux Line Lattice, *Phys. Rev. Lett.* **74**, 3029 (1995).
- [46] W. Henderson, E. Y. Andrei, M. J. Higgins, and S. Bhattacharya, Metastability and Glassy Behavior of a Driven Flux-Line Lattice, *Phys. Rev. Lett.* **77**, 2077 (1996).
- [47] S. S. Banerjee, N. G. Patil, S. Ramakrishnan, A. K. Grover, S. Bhattacharya, P. K. Mishra, G. Ravikumar, T. V. Chandrasekhar Rao, V. C. Sahni, M. J. Higgins, C. V. Tomy, G. Balakrishnan, and D. McK. Paul, Disorder, metastability, and history dependence in transformations of a vortex lattice, *Phys. Rev. B* **59**, 6043 (1999).
- [48] K. Ghosh, S. Ramakrishnan, A. K. Grover, G. I. Menon, G. Chandra, T. V. Chandrasekhar Rao, G. Ravikumar, P. K. Mishra, V. C. Sahni, C. V. Tomy, G. Balakrishnan, D. Mck Paul, and S. Bhattacharya, Reentrant Peak Effect and Melting of a Flux Line Lattice in 2H-NbSe_2 , *Phys. Rev. Lett.* **76**, 4600 (1996).
- [49] C. Tang, X. S. Ling, S. Bhattacharya, and P. M. Chaikin, Peak effect in superconductors: Melting of Larkin domains, *Europhys. Lett.* **35**, 597 (1996).
- [50] Y. Wang, J. Wang, T. Kitamura, H. Hirakata, and T. Shimada, Exponential Temperature Effects on Skyrmion-Skyrmion Interaction, *Phys. Rev. Appl.* **18**, 044024 (2022).
- [51] A. E. Koshelev and V. M. Vinokur, Dynamic Melting of the Vortex Lattice, *Phys. Rev. Lett.* **73**, 3580 (1994).
- [52] M. C. Hellerqvist, D. Ephron, W. R. White, M. R. Beasley, and A. Kapitulnik, Vortex Dynamics in Two-Dimensional Amorphous $\text{Mo}_{77}\text{Ge}_{23}$ Films, *Phys. Rev. Lett.* **76**, 4022 (1996).
- [53] B. L. Brown, U. C. Täuber, and M. Pleimling, Skyrmion relaxation dynamics in the presence of quenched disorder, *Phys. Rev. B* **100**, 024410 (2019).
- [54] J. Stidham and M. Pleimling, Late stages in the ordering of magnetic skyrmion lattices, *Phys. Rev. B* **102**, 144434 (2020).
- [55] Y. Zhou, R. Mansell, T. Ala-Nissila, and S. van Dijken, Thermal motion of skyrmion arrays in granular films, *Phys. Rev. B* **104**, 144417 (2021).
- [56] Y. Ge, J. Rothörl, M. A. Brems, N. Kerber, R. Gruber, T. Dohi, M. Kläui, and P. Virnau, Constructing coarse-grained skyrmion potentials from experimental data with Iterative Boltzmann Inversion, *Commun. Phys.* **6**, 30 (2023).
- [57] P. Le Doussal and T. Giamarchi, Moving glass theory of driven lattices with disorder, *Phys. Rev. B* **57**, 11356 (1998).
- [58] C. Reichhardt and C. J. O. Reichhardt, Nonlinear transport, dynamic ordering, and clustering for driven skyrmions on random pinning, *Phys. Rev. B* **99**, 104418 (2019).
- [59] U. Yaron, P. L. Gammel, D. A. Huse, R. N. Kleiman, C. S. Oglesby, E. Bucher, B. Batlogg, D. J. Bishop, K. Mortensen, and K. N. Clausen, Structural evidence for a two-step process in the depinning of the superconducting flux-line lattice, *Nature (London)* **376**, 753 (1995).
- [60] L. Balents, M. C. Marchetti, and L. Radzihovsky, Nonequilibrium steady states of driven periodic media, *Phys. Rev. B* **57**, 7705 (1998).
- [61] F. Pardo, F. de la Cruz, P. L. Gammel, E. Bucher, and D. J. Bishop, Observation of smectic and moving-Bragg-glass phases in flowing vortex lattices, *Nature (London)* **396**, 348 (1998).
- [62] C. J. Olson, C. Reichhardt, and F. Nori, Nonequilibrium Dynamic Phase Diagram for Vortex Lattices, *Phys. Rev. Lett.* **81**, 3757 (1998).
- [63] C. Reichhardt, C. J. Olson, N. Grønbech-Jensen, and F. Nori, Moving Wigner Glasses and Smectics: Dynamics of Disordered Wigner Crystals, *Phys. Rev. Lett.* **86**, 4354 (2001).
- [64] G. Li, E. Y. Andrei, Z. L. Xiao, P. Shuk, and M. Greenblatt, Onset of Motion and Dynamic Reordering of a Vortex Lattice, *Phys. Rev. Lett.* **96**, 017009 (2006).
- [65] L. Liu, W. Chen, and Y. Zheng, Current-Driven Skyrmion Motion Beyond Linear Regime: Interplay between Skyrmion Transport and Deformation, *Phys. Rev. Appl.* **14**, 024077 (2020).
- [66] M. Weißenhofer, L. Rózsa, and U. Nowak, Skyrmion Dynamics at Finite Temperatures: Beyond Thiele's Equation, *Phys. Rev. Lett.* **127**, 047203 (2021).